ANALYTICAL SCIENCES MARCH 2015, VOL. 31

Label-free Electrochemical Detection of the Human Adenovirus 40/41 Fiber Gene

Min-Jung SONG* and Joon-Hyung JIN†**

**Department of Materials Science and Engineering, Yonsei University, 50 Yonsei-ro, Seodaemun-gu, Seoul 120–749, Korea*
***Department of Mechanical Engineering, Korea University, 1, 5-Ga, Anam-dong, Seoungbuk-gu, Seoul 136–713, Korea*

A nanoporous silicon-based label-free DNA biosensor was fabricated to monitor rapidly enteric adenovirus types 40 and 41, a leading cause of viral gastroenteritis in children. Nanoporous silicon (NPS) was formed by an anodic etching process in a mixture solution containing hydrofluoric acid and ethanol. The polypyrrole (PPy) film was directly electropolymerized on The NPS substrate. Twenty-five base pairs of probe DNA (pDNA), derived from the fiber gene, was electrochemically doped on the PPy-coated NPS substrate. The conductivity change due to the immobilized pDNA and hybridized target DNA (tDNA) was expressed as an arbitrary factor, γ, which is a normalized numerical term used for the selective quantification of the tDNA. γ was inversely proportional to the concentration of complementary tDNA, but independent of the non-complementary tDNA. The sensitivity slope for detecting $tDNA_c$ was $-1.54\ \mu M^{-1}$, based on the factor γ in the range of 0.4 to 1.0 μM of tDNA. The surface roughness was characterized using atomic force microscopy.

Keywords Direct electropolymerization, coulometric DNA sensor, human adenovirus, nanoporous silicon

(Received September 16, 2014; Accepted January 29, 2015; Published March 10, 2015)

Introduction

DNA biosensors have attracted considerable attention due to their potential applications, such as clinical diagnostics, gene analysis, forensics, food safety inspection, environmental monitoring, and biowarfare target detection.[1–4] Among the various DNA sensors, electrochemical DNA (E-DNA) sensors have been developed owing to their significant advantages of high sensitivity and selectivity, simple and portable instrumentation, fast response and low cost.[1,2,5] These sensors can be categorized into two types: labeled and label-free E-DNA sensors. The labeled E-DNA sensors employ a variety of labels and markers for better detection limits, but involve complicated steps and require a longer processing time. Label-free E-DNA sensors exhibit lower sensitivity than the labeled sensors albeit requiring no additional reagents and pre-/post-hybridization steps.[5] Many researchers have tried to develop label-free E-DNA sensors with high sensitivity using various platforms.[6-9] Porous silicon (PS) has been predominantly used as an active platform for biochemical sensing devices due to its large surface area-to-volume ratio and rough surface for biological immobilization, which leads to the enhanced sensitivity.[10] In addition, PS is simply produced by an electrochemical etching process of crystalline silicon in a solution of hydrofluoric acid (HF). Its morphological properties can be easily controlled by adjusting the etching parameters (*e.g.*, HF concentration, silicon type, doping level, current density, anodization time and temperature).[11]

Polypyrrole (PPy) is one of the most extensively exploited conducting polymers as an excellent tool for the immobilization of biomolecules, such as enzyme, antibody, or DNA, because it exhibits high electrical conductivity, and high stability in air and in aqueous media.[12] The polymer is usually synthesized by electrochemical polymerization and its properties, including shape, thickness, and conductivity, can be controlled by adjusting the electrolyte, deposition current, deposition potential and time.[13]

In this work, we developed a label-free DNA sensor based on nanoporous silicon (NPS) with polypyrrole (PPy) for the rapid detection of Human Adenoviruses (HAdV) 40/41. Here, HAdV 40/41 emerging waterborne viruses associated with gastroenteritis in infants and children[14,15] were the detection targets. The NPS layer was formed on a low-resistivity p-type silicon (p-Si) wafer through an anodic etching process, and the polypyrrole (PPy) film was directly electropolymerized on the NPS layer. A DNA probe (pDNA), which is specific to the fiber gene of HAdV 40/41, was immobilized on the PPy film. Complementary target DNA ($tDNA_c$) and non-complementary target DNA ($tDNA_{nonc}$) strands were hybridized on the pDNA-immobilized NPS chips, and a normalization factor (γ) was introduced to standardize sensor-to-sensor fabrication variability.

† To whom correspondence should be addressed.
E-mail: jjh1023@chol.com; jjh1023@korea.ac.kr

Experimental

Reagents and chemicals

A pyrrole monomer and a 70% solution of $HClO_4$ (Aldrich Chemical Co., WI) were used to produce PPy by electropolymerization. A Milli-Q pure water system was used for the preparation of deionized water (DI water). $KClO_4$ (99.99%) (Aldrich Chemical Co.) was used as a supporting electrolyte of all aqueous media. Ethanol (99.5%, Aldrich Chemical Co.) was used for etchant preparation and a provisional storage of the NPS substrate prior to annealing.

A quikhyb® hybridization solution (Stratagene, CA) was used for the hybridization of $tDNA_c$ and $tDNA_{nonc}$ to the pDNA. All reagents were used without further purification. A 25-bp pDNA sequence, 5′-AACATGCTCATCCAAATCTCGCCTA-3′, for detecting the fiber gene of HAdV 40/41 was selected from the literature.[16] The pDNA sequence lies within the conserved regions of the fiber gene, and is highly specific to HAdV 40/41. Oligonucleotides were synthesized for use as $tDNA_c$ (5′-TAGG CGAGATTTGGATGAGCATGTT-3′) and as $tDNA_{nonc}$ (5′-AGA AATCTCGAGTCGGAGATGCAGG-3′). The pDNA concentration was determined using a Nanodrop ND-1000 instrument following the manufacturer's instructions (Nanodrop, Wilmington, DE). The desired concentration of DNA for this study was obtained by dilution in nuclease-free water (Eppendorf). Adequate amounts of tDNA solution were mixed with a Quikhyb® solution to prepare tDNA standard solutions.

Apparatus

Electrochemical measurements were performed in an electrochemical workstation composed of a potentiostat/galvanostat (Princeton Applied Research, Model 263A), N_2 gas bubbling/purging system, and a Teflon electrochemical cell. Pt wire (99.99%) counter electrode and a double junction Ag/AgCl (Aldrich Chemical Co., WI) reference electrode were used. A Pt tip was used as the quasi-reference electrode (QRE) for the electropolymerization of PPy in an acetonitrile (EMD Science) solvent. A JSM-6300F scanning microscope (JEOL, Japan) was used to obtain scanning electron microscopy (SEM) images with the pre-deposition of a 10 nm osmium layer using Pure Osmium Coater (Neoc-An, Japan). Contact-mode atomic-force microscopy (AFM; Nano Scope III, Digital Instruments, CA) was used to measure the surface roughness.

Fabrication of NPS-based DNA sensor

A boron-doped, one-side-polished p-Si wafer (0.01 - 0.02 Ω cm, 100 orientation, Montco Silicon Technologies, Inc., PA) was employed as a substrate. A 19 × 19 mm silicon chip (1.5 cm^2) was dipped in a 48% HF solution for several seconds to remove the natural oxide layer, and was then rinsed with DI water. After drying with N_2 gas, the chip was placed in a custom-made Teflon electrochemical cell (Fig. S1, Supporting Information), and a current density (J) of –5 mA cm^2 was applied to the cell for 30 min. The etchant was a 14.4% HF solution (30 mL of 48% HF + 70 mL of 100% ethanol). Once the NPS layer was formed, the substrate was annealed at 110ºC for 1 h. Then, the PPy film was directly electropolymerized on the NPS layer in a non-aqueous media. After rinsing with pure CH_3CN, the PPy-coated NPS substrate (NPS/PPy) was dried at ambient temperature. Then, the pDNA strands were chronoamperometrically doped into the PPy film by applying 0.6 V *vs.* Pt (QRE) for 20 min to form pDNA-doped NPS/PPy (NPS/PPy+pDNA). The pDNA doping solution contained 0.01 M $KClO_4$ and 10 nM pDNA. One hundred microliters each $tDNA_c$ and $tDNA_{nonc}$ solution was loaded on the NPS/PPy+pDNA substrate and hybridized at 60ºC in a water bath for 1 h to obtain the tDNA-hybridized NPS/PPy+pDNA substrate (NPS/PPy+pDNA+tDNA).[17] All substrates prepared for electrochemical characterization were thoroughly cleaned before use with saline-sodium citrate buffer (SSC, 0.1X, 0.2 µm filtered) containing 0.1% (w/v) sodium dodecyl sulfate (SDS) solution, and vortexed at 3000 rpm for 10 s.

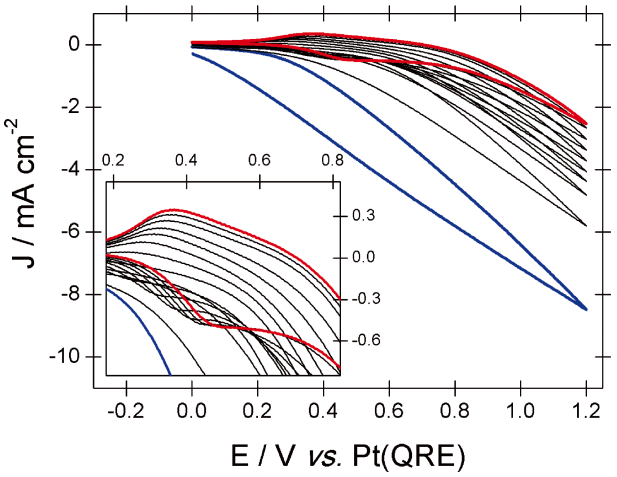

Fig. 1 Electropolymerization of pyrrole on an NPS substrate in an acetonitrile solution containing 0.02 M pyrrole and 0.1 M $HClO_4$ by applying 10 times of potential scanning at 0 – 1.2 V *vs.* Pt (QRE). The scan rate was 25 mV s^{-1}. Blue and red solid lines denote the first and tenth CV diagrams, respectively.

Results and Discussion

A silicon wafer is a good substrate for the direct electropolymerization of pyrrole without using any metallic underlayer as long as the resistivity of the silicon wafer is low enough for supplying sufficient electrical charge. However, the hydrophilic PPy film electropolymerized on the hydrophobic bare silicon surface spontaneously detaches from the silicon surface. NPS can be used as an alternative surface for the direct deposition of PPy. In addition to its large surface-to-volume ratio, NPS is easily oxidized to form a hydrophilic silicon dioxide (SiO_2) layer under atmospheric conditions. The contact angle of SiO_2 with pure water is *ca.* 20°, and the root-mean-square (rms) value of the surface roughness is comparable to that of a polished silicon wafer.[18] Even though a freshly prepared NPS surface is more hydrophobic than bare Si (water contact angle > 95°),[19] it is quite sensitive to air, and thus wafer annealing after NPS formation promotes growth of SiO_2 on a top of the NPS substrate. The NPS surface formed by electrochemical anodization and subsequent annealing maintains hydrophilic property for a longer period of time than the conventional O_2 plasma-based surface modification,[20] and has a relatively high surface free energy due to the increased hydrophilicity.[21] A macroporous silicon (MPS, pore diameter = 2 µm and pore depth = 10 µm) layer was unfavorable for direct deposition of PPy (Fig. S2, Supporting Information).

Figure 1 shows cyclic voltammograms (CV diagrams) of the direct electropolymerization of PPy on the NPS substrate. The electropolymerization of pyrrole on a noble metal substrate requires *ca.* 0.6 V bias. NPS substrates, however, require

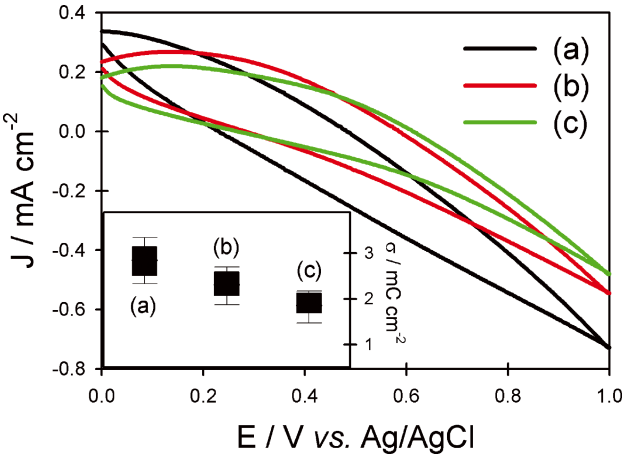

Fig. 2 CV diagrams of (a) NPS/PPy, (b) NPS/PPy+pDNA, and (c) NPS/PPy+pDNA+tDNA in an aqueous solution containing 0.01 M $KClO_4$. Scan rate was 50 mV s^{-1}. The tDNA concentration was 0.6 μM. The box plot shown in the inset summarizes charge density variations obtained from (a), (b), and (c) substrates. Ten, eight, and seven data points were used to determine the average charge densities and standard deviations for the (a), (b), and (c) substrates, respectively.

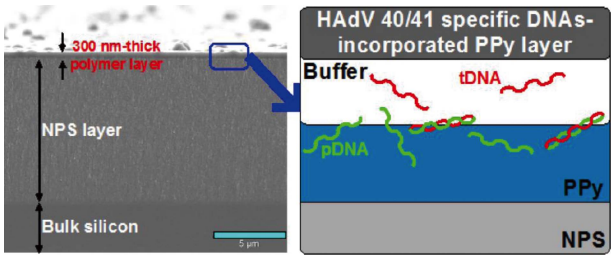

Fig. 3 Cross-sectional SEM image and schematic drawing of the multi-layered NPS/PPy+pDNA+tDNA substrate.

additional potential energy for direct electropolymerization. Although the silicon substrate used in this study has low resistivity, its resistance is still three orders of magnitude larger than that of platinum. The intrinsic resistance of the NPS layer is another reason for the high-energy requirement. In some cases, the NPS layer can even be used as a passivation layer.[22] As shown in Fig. 1, the charging current (I_c) increased between 0.2 and 0.8 V, meaning that PPy film was growing on the NPS substrate. No appreciable amount of I_c increase was observed in the case of the MPS or bare silicon substrates.

DNA fragments are attracted to the positively-charged electrode substrate, and are electrostatically adsorbed on the surface due to the intrinsic negatively charged phosphate backbone of nucleotides.[23] A 25-bp pDNA from HAdV 40/41 was chronoamperometrically doped into the PPy film on an NPS substrate, as shown in Fig. S3 (Supporting Information). Even though guanine is the most oxidizable DNA base,[24] the guanine bases covalently bound to deoxyribose groups of the DNA backbone are more stable than free guanines in a wide range of the applied potential, and the labeling of DNA strands with electro-active species is essential for the faradaic current-based quantification of the DNA.[25] Nevertheless, 0.6 V *vs.* Pt (QRE) of relatively low potential was applied for pDNA immobilization in order to minimize any unwanted oxidation of DNA bases, which can restrict hydrogen bonding between complementary DNA strands. Once pDNAs were successfully doped into the positively charged PPy network, the pDNAs and the PPy were bound together electrostatically. Even though, in the following cyclic voltammetry (CV) measurement, the NPS/PPy+pDNA may experience a more extreme condition than in the previous pDNA doping process, the exposure time of the electrode to a voltage higher than 0.6 V in the CV is only 16 s, which is a reasonably short period of time, and any damage to the NPS/PPy+pDNA will be negligible. Note that guanine bases involved in hydrogen bonding by hybridization are thermodynamically more stable, and therefore more resistive to undesirable irreversible oxidation in the CV measurement than free quanine bases.

Figure 2 shows cyclic voltammograms of NPS/PPy, NPS/PPy+pDNA, and NPS/PPy+pDNA+tDNA electrodes. Because no redox-active species, except trace impurities, have been used to modify the working electrode, the dominant current flows are caused by the non-faradaic process, including the pseudocapacitive behavior. Conducting polymers such as polyaniline, polyethylenedioxythiophene, and PPy are frequently-used electrode materials of electrochemical capacitors for enhancing the pseudocapacitance.[26,27] It can be assumed that the amount of electric charge in the form of a structure-involved pseudocapacitance remains unchanged, considering that the NPS/PPy is the common basic electrode substrate in this work, and the doped DNA is the major factor affecting the amount of current flow. The electrode capacitance increases after pDNA-immobilization, and further enhances upon tDNA-hybridization. This is confirmed by the box plot shown in the inset of Fig. 2, indicating a decrease in the charge density of the PPy film as the pDNA and subsequently the tDNA strands are doped into the film. Note that the potential scan rate and the working electrode area are fixed known values, and the charge densities can be determined by integration of the CV diagrams.

Enhanced wettability by the ethanol component in the silicon etchant makes it easier to grow a homogenous NPS layer.[28] Due to the large surface area and the possibility of spontaneous oxidation to form a hydrophilic silicon dioxide layer, the NPS surface is an excellent substrate for preparing a metal-free conducting polymer-modified electrode. The uppermost layer of the SEM image shown in Fig. 3 is an actual sensing film composed of PPy and pDNA with a thickness of *ca.* 300 nm. Both the NPS and bulk silicon layers act as pathways for the electrical signal coming from the sensing layer. Compared with the signal from a metallic thin-film, a semiconductor electrode might provide a better signal-to-noise ratio along with the added advantage of a shorter fabrication process resulting from omission of the metal deposition step. In general, a negligible band-gap of a metal makes it very hard to avoid noise interference, whereas, in a semiconductor the larger energy difference between valence and conduction bands can play a role in noise filtration. Chronoamperometrically doped pDNA and the subsequently hybridized tDNA may alter the charge density of the PPy-based sensing film. The maximum doping level of perchlorate anion in the PPy film is about 33%.[29] This means one perchlorate per three monomer units, and the 25-bp pDNA strand needs at least 225 pyrrole monomers to envelop the pDNA if it is assumed that the amount of charge carried by phosphate and perchlorate anions is the only difference between the two anions. However, the doped amount of the pDNA is still unpredictable because the anion doping might not be uniform due to the non-ideal structure of conventional conducting polymer film.[29]

The AFM images (Fig. S4, Supporting Information) show that

the surface roughness (r_s) of the NPS/PPy was 31.1 nm in rms value when the scan rate and size were 25 Hz and 15 μm × 15 μm, respectively. The rms value of NPS/PPy+pDNA was 24.8 nm, *i.e.*, a 20.3% decrease compared with NPS/PPy. After the hybridization of $tDNA_c$, the rms value of the NPS/PPy+pDNA+$tDNA_c$ decreased by 39.2% from that of NPS/PPy. However, there was no notable difference in the rms values of the NPS/PPy+pDNA+$tDNA_c$ and NPS/PPy+pDNA+$tDNA_{nonc}$ substrates. Normally, the conductive PPy film is positively charged and anions in the electrolyte used for electropolymerization of the PPy neutralize the positively charged polymer backbone. Some $tDNA_{nonc}$ strands can also be attracted to the PPy film. This nonspecific adsorption of tDNA strands is due to the electron-rich phosphate groups in the DNA backbone.

A dimensionless factor, γ, was introduced as the normalization factor for correcting variations between the sensing electrodes, and it was employed to calibrate each sensing electrode after tDNA hybridization. Factor γ is defined as the ratio of the charge density difference between PPy+pDNA+tDNA and bare PPy to that between PPy+pDNA and bare PPy, as represented by

$$\gamma = \frac{\sigma_{NPS/PPy} - \sigma_{NPS/PPy+pDNA+tDNA}}{\sigma_{NPS/PPy} - \sigma_{NPS/PPy+pDNA}} = \frac{d\sigma_x}{d\sigma_y}, \quad (1)$$

where $\sigma_{NPS/PPy}$, $\sigma_{NPS/PPy+pDNA}$, and $\sigma_{NPS/PPy+pDNA+tDNA}$ are the charge densities of the NPS/PPy, NPS/PPy+pDNA, and NPS/PPy+pDNA+tDNA substrates, respectively. The charge density could be directly obtained from the CV diagrams by integrating J over the elapsed time (Fig. 2). The potential axis can be converted into the time domain by dividing the potential by the scan rate used. If $d\sigma_x$ and $d\sigma_y$ are defined as $(\sigma_{NPS/PPy} - \sigma_{NPS/PPy+pDNA+tDNA})/\sigma_{NPS/PPy}$ and $(\sigma_{NPS/PPy} - \sigma_{NPS/PPy+pDNA})/\sigma_{NPS/PPy}$, respectively, the values of $d\sigma_x$ and $d\sigma_y$ are between 0 and 1. This is because the magnitude of the charge density for each substrate is in the order $\sigma_{NPS/PPy} > \sigma_{NPS/PPy+pDNA} > \sigma_{NPS/PPy+pDNA+tDNA}$ in accordance with the assumption that DNA is an insulator. Therefore, the factor γ (= $d\sigma_x/d\sigma_y$) is larger than 1 due to $d\sigma_x$ being larger than $d\sigma_y$.

In contrast, Fig. 4 shows a gradual decrease in the factor γ with an increase in the $tDNA_c$ concentration. γ eventually becomes smaller than 1 at 1.0 μM of $tDNA_c$ (the molar concentration of $tDNA_c$ and $tDNA_{nonc}$ derived from the exact molecular weights of nucleotides are 7933 and 7921, respectively). If we assume that all NPS/PPy+pDNA substrates are electrochemically identical, $d\sigma_y$ is constant. This leads to the conclusion that $d\sigma_x$ decreases with increasing $tDNA_c$ concentration, causing the factor γ to decrease. Furthermore, $\gamma < 1$ signifies that an NPS/PPy+pDNA substrate becomes more conductive after being hybridized with $tDNA_c$. This is explained by the conductivity difference between the ssDNA and dsDNA strands, *i.e.*, dsDNA is more conductive than ssDNA. Nagaoka *et al.* inferred that the resistance of dsDNA immobilized between nanogapped Au films depends nonlinearly on the number of mismatched DNA base pairs.[30] Even though the enhanced conductivity in dsDNA is mainly due to its reduced resistance along the long axis,[31] it was not a crucial factor herein because the pDNA electrostatically doped into the PPy film could not be highly ordered. It is not the anisotropic orientation, but rather the amount of dsDNA inside the PPy film, that is of significance in this case. In general, a conducting polymer is considered to be a semiconductor, and dsDNA, in this case, is a dopant. A highly doped conducting polymer film will be more conductive. The sensitivity based on the normalization factor γ of the NPS/PPy+pDNA+$tDNA_c$ was −1.48 μM^{-1} in the linear range of 0.1 – 1.0 μM of $tDNA_c$, while that of the NPS/PPy+pDNA+$tDNA_{nonc}$ was 7.7×10^{-4} μM^{-1} in the same range of $tDNA_{nonc}$. This implied that the correctly-hybridized dsDNA was more conductive than the non-complementary ssDNA. This is potentially due to the π-stacking between adjacent nucleotides along the molecules.[32,33] The lowest concentration of tDNA used in this study was 0.1 μM, which is equivalent to 6.0×10^{12} copies. The actual concentrations of HAdV 40/41 in real wastewater samples are lower (up to 10^7 copies L^{-1}).[34,35] The independence of the γ factor on $tDNA_{nonc}$ concentration also indicates the higher conductivity of a well-matched dsDNA strand than that of a mismatched strand.

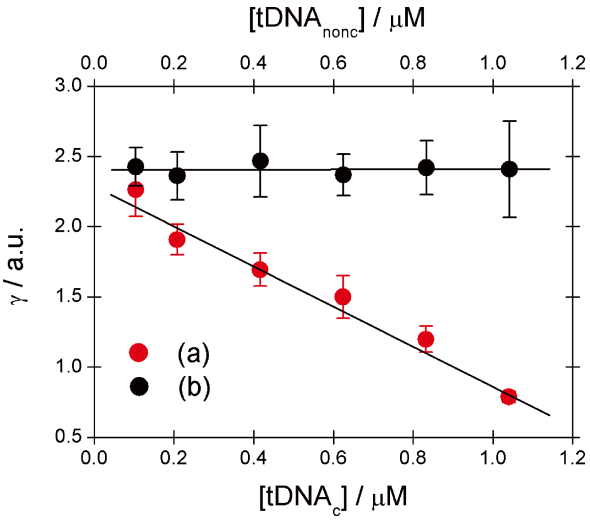

Fig. 4 Calibration curves of NPS/PPy+pDNA+$tDNA_c$ (a), and NPS/PPy+pDNA+$tDNA_{nonc}$ (b). Linear slopes corresponding to the closed red and the close black circles are −1.48 μM^{-1} and 7.7×10^{-4} μM^{-1}, respectively. Three data points were used to calculate the average γ and the standard deviations at a given tDNA concentration.

Conclusions

In conclusion, the large surface area, enhanced roughness, and increased hydrophilicity of the NPS surface formed on a low-resistivity p-Si by electrochemical anodization collectively allows the direct electropolymerization of pyrrole on the silicon substrate. Owing to the direct deposition of PPy on the silicon substrate without using any metallic thin-film, the fabrication costs are expected to be minimal, and the fabrication procedure itself simplified. The label-free coulometric DNA sensor based on a PPy-coated NPS platform enables portable operation without requiring any complex equipment, data analysis, or sample preparation steps. The arbitrary factor, γ, introduced to normalize the sensor-to-sensor variation, decreased with increasing $tDNA_c$ concentration. The sensitivity of the NPS/PPy+pDNA+$tDNA_c$ was higher than that of the NPS/PPy+pDNA+$tDNA_{nonc}$. The immediate application of this biosensor is for near real-time measurements of CPEs after cell culture, and also for direct applications to environmental samples without requiring the cell culture step. Label-free electrochemical detection at subpico-level concentrations requires rapid quantification of a field sample of HAdV 40/41 without any polymerase chain reaction (PCR) amplification. Therefore, further optimization is needed for enhanced

sensitivity. This work therefore provides proof-of-principle with promising performance characteristics.

Acknowledgements

This study was supported by the Priority Research Centers Program (2009-0093823) through the National Research Foundation of Korea (NRF).

Supporting Information

This material is available free of charge on the Web at http://www.jsac.or.jp/analsci/.

References

1. B. C. Yin, Y. M. Guan, and B. C. Ye, *Chem. Commun.*, **2012**, *48*, 4208.
2. H. L. Jin, M. Wei, and J. S. Wang, *Chem. Cent. J.*, **2013**, 7.
3. H. T. Ngo, H. N. Wang, A. M. Fales, and T. Vo-Dinh, *Anal. Chem.*, **2013**, *85*, 6378.
4. J. L. Lopez-Paz, M. A. Gonzalez-Martinez, J. Escorihuela, M. J. Banuls, R. Puchades, and A. Maquieira, *Sens. Actuators, B*, **2014**, *192*, 221.
5. T. G. Drummond, M. G. Hill, and J. K. Barton, *Nat. Biotechnol.*, **2003**, *21*, 1192.
6. L. A. Thompson, J. Kowalik, M. Josowicz, and J. Janata, *J. Am. Chem. Soc.*, **2003**, *125*, 324.
7. H. Peng, C. Soeller, N. Vigar, P. A. Kilmartin, M. B. Cannell, G. A. Bowmaker, R. P. Cooney, and J. Travas-Sejdic, *Biosens. Bioelectron.*, **2005**, *20*, 1821.
8. K. J. Huang, Y. J. Liu, H. B. Wang, and Y. Y. Wang, *Electrochim. Acta*, **2014**, *118*, 130.
9. R. M. Kong, Z. L. Song, H. M. Meng, X. B. Zhang, G. L. Shen, and R. Q. Yu, *Biosens. Bioelectron.*, **2014**, *54*, 442.
10. A. Jane, R. Dronov, A. Hodges, and N. H. Voelcker, *Trends Biotechnol.*, **2009**, *27*, 230.
11. H. Foll, M. Christophersen, J. Carstensen, and G. Hasse, *Mater. Sci. Eng., R*, **2002**, *39*, 93.
12. N. C. Foulds and C. R. Lowe, *J. Chem. Soc., Faraday Trans. 1*, **1986**, *82*, 1259.
13. K. M. Cheung, D. Bloor, and G. C. Stevens, *Polymer*, **1988**, *29*, 1709.
14. M. J. Albert, A. S. G. Faruque, S. M. Faruque, R. B. Sack, and D. Mahalanabis, *J. Clin. Microbiol.*, **1999**, *37*, 3458.
15. F. Bon, P. Fascia, M. Dauvergne, D. Tenenbaum, H. Planson, A. M. Petion, P. Pothier, and E. Kohli, *J. Clin. Microbiol.*, **1999**, *37*, 3055.
16. K. Pehler-Harrington, M. Khanna, C. R. Waters, and K. J. Henrickson, *J. Clin. Microbiol.*, **2004**, *42*, 4072.
17. D. S. Lindsay, D. S. Zarlenga, H. R. Gamble, F. AlYaman, P. C. Smith, and B. L. Blagburn, *J. Parasitol.*, **1995**, *81*, 920.
18. T. Sordel, F. Kermarec-Marcel, S. Garnier-Raveaud, N. Glade, F. Sauter-Starace, C. Pudda, M. Borella, M. Plissonnier, F. Chatelain, F. Bruckert, and N. Picollet-D'hahan, *Biomaterials*, **2007**, *28*, 1572.
19. S. P. Low, K. A. Williams, L. T. Canham, and N. H. Voelcker, *Biomaterials*, **2006**, *27*, 4538.
20. S. Bhattacharya, Y. F. Gao, V. Korampally, M. T. Othman, S. A. Grant, K. Gangopadhyay, and S. Gangopadhyay, *Appl. Surf. Sci.*, **2007**, *253*, 4220.
21. I. Piwonski and A. Ilik, *Appl. Surf. Sci.*, **2006**, *253*, 2835.
22. A. O. Konstantinov, C. I. Harris, A. Henry, and E. Janzen, *Mater. Sci. Eng., B*, **1995**, *29*, 114.
23. J. Fritz, E. B. Cooper, S. Gaudet, P. K. Sorger, and S. R. Manalis, *Proc. Natl. Acad. Sci. U. S. A.*, **2002**, *99*, 14142.
24. K. Arora, A. Chaubey, R. Singhal, R. P. Singh, M. K. Pandey, S. B. Samanta, B. D. Malhotra, and S. Chand, *Biosens. Bioelectron.*, **2006**, *21*, 1777.
25. J. K. Wu, C. H. Huang, G. F. Cheng, F. Zhang, P. G. He, and Y. Z. Fang, *Electrochem. Commun.*, **2009**, *11*, 177.
26. G. A. Snook, P. Kao, and A. S. Best, *J. Power Sources*, **2011**, *196*, 1.
27. F. Alvi, M. K. Ram, P. A. Basnayaka, E. Stefanakos, Y. Goswami, and A. Kumar, *Electrochim. Acta*, **2011**, *56*, 9406.
28. M. du Plessis, *Sens. Actuators, A*, **2007**, *135*, 666.
29. P. Chandrasekhar, "*Conducting polymers, fundamentals and applications: a practical approach*", xxxvi, **1999**, Kluwer Academic, Boston.
30. H. Shiigi, S. Tokonami, H. Yakabe, and T. Nagaoka, *J. Am. Chem. Soc.*, **2005**, *127*, 3280.
31. Y. Okahata, T. Kobayashi, K. Tanaka, and M. Shimomura, *J. Am. Chem. Soc.*, **1998**, *120*, 6165.
32. H. W. Fink and C. Schonenberger, *Nature*, **1999**, *398*, 407.
33. D. Porath, A. Bezryadin, S. de Vries, and C. Dekker, *Nature*, **2000**, *403*, 635.
34. S. Choi and S. C. Jiang, *Appl. Environ. Microbiol.*, **2005**, *71*, 7426.
35. J. W. He and S. Jiang, *Appl. Environ. Microbiol.*, **2005**, *71*, 2250.